

Liver Lesion Extraction with Fuzzy Thresholding in Contrast Enhanced Ultrasound Images

Abder-Rahman Ali, Adélaïde Albouy-Kissi, Manuel Grand-Brochier, Viviane Ladan-Marcus, Christine Hoeffl, Claude Marcus, Antoine Vacavant, Jean-Yves Boire

Abstract—In this paper, we present a new segmentation approach for focal liver lesions in contrast enhanced ultrasound imaging. This approach, based on a two-cluster Fuzzy C-Means methodology, considers type-II fuzzy sets to handle uncertainty due to the image modality (presence of speckle noise, low contrast, etc.), and to calculate the optimum inter-cluster threshold. Fine boundaries are detected by a local recursive merging of ambiguous pixels. The method has been tested on a representative database. Compared to both Otsu and type-I Fuzzy C-Means techniques, the proposed method significantly reduces the segmentation errors.

Keywords—Defuzzification, fuzzy clustering, image segmentation, type-II fuzzy sets.

I. INTRODUCTION

CONTRAST Enhanced UltraSound (CEUS) [1]-[3] consists in acquiring an ultrasound image after injecting in the patient's blood a contrast agent made of gas-filled microbubbles [4]. This new modality allows an improvement of tumor detection by emphasizing the relative differential perfusion of the tumor tissue compared to normal liver parenchyma. Unfortunately, the modality suffers, as conventional ultrasonology, from several drawbacks, making the lesion detection process very difficult: low resolution, low contrast between the lesion and the surrounding tissue, and discontinuity [4].

Many techniques have been developed for ultrasound image segmentation. They are categorized into: histogram thresholding; region growing; model-based (active contour, level set; Markov model), machine learning; watershed methods; and fuzzy clustering [5]-[9]. Due to the complex nature of images, the use of these methodologies often involves preprocessing (filtering for noise reduction), and/or prior knowledge.

In this paper, we present a new liver lesion segmentation approach for CEUS imaging that considers two clusters: the lesion and the surrounding tissue. Fuzzy C-Means clustering is

used due to its ability to deal with different types of uncertainty and treat overlapping clusters. This method considers both local and global information. The optimum inter-cluster threshold is calculated by considering type-II fuzzy sets, an extension of type-I fuzzy sets, but with an additional dimension that represents the uncertainty about the degree of membership. Type-II fuzzy sets are considered useful in circumstances where it is difficult to determine the exact membership function for a fuzzy set [10], and they can be used to enhance the contrast of ultrasound images [10-11]. Such optimum threshold enables the detection of “ambiguous pixels” close to the boundary regions. Their cluster affection is done by applying a two-step decision that simulates gradual focusing perception, thus considering the local information.

The paper is organized as follows: Section II provides a detailed explanation of the proposed approach, in addition to type-I fuzzy sets, type-II fuzzy sets, and the decision process; Section III shows the results and evaluations of the proposed methodology; and the paper is concluded in Section IV.

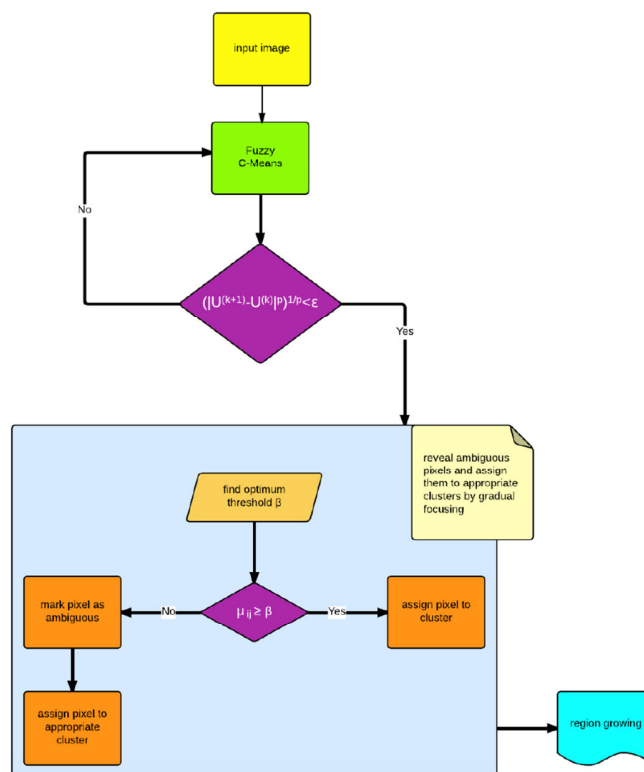


Fig. 1 Proposed methodology

Abder-Rahman Ali is with ISIT, Université d'Auvergne, UMR/CNRS/6284, BP10448, F-63000 Clermont-Ferrand, France (phone: 06-524-18395; e-mail: abder-rahman.ali@etu.udamail.fr).

Adélaïde Albouy-Kissi, Manuel Grand-Brochier, Antoine Vacavant, and Jean-Yves Boire are with ISIT, Université d'Auvergne, UMR/CNRS/6284, BP10448, F-63000 Clermont-Ferrand, France (e-mail: adelaid.kissi@udamail.fr, manuel.grandbrochier@udamail.fr, antoine.vacavant@udamail.fr, j-yves.boire@udamail.fr).

Viviane Ladan-Marcus, Christine Hoeffl, and Claude Marcus are with CHU Reims Service de Radiologie, Hospital Robert Debré, Avenue du Général Koenig 51100 Reims, France (e-mail: vladammarcus@chu-reims.fr, choeffel-formes@chu-reims.fr, cmarcus@chu-reims.fr).

II. METHODOLOGY

The proposed approach, illustrated in Fig. 1, consists of the following main parts: (i) Fuzzy C-Means clustering; (ii) calculating the optimum threshold (inter-cluster threshold) that distinguishes between the ambiguous pixels and non-ambiguous pixels; (iii) revealing ambiguous pixels; (iv) local treatment of ambiguous pixels; and (v) final segmentation.

A. Type-I Fuzzy Sets

The concept of fuzzy sets was introduced as a generalization of the classic set theory. In real world, many classes of objects are not as well defined as regular set theory would suggest, and thus, the concept of a crisp set could be very hard to deal with sometimes. The definition of a fuzzy set has what is needed to define a set with inexact boundaries *i.e.* objects with vague membership. A fuzzy set A in X can be defined as a set of ordered pairs [11]:

$$A = \{(x, y) | x \in X, y = \mu_A(x) \in [0, 1]\} \quad (1)$$

where $\mu_A(x)$ is the membership function.

Under these considerations, we can describe the type-I Fuzzy C-Means clustering.

Let $X = \{x_1, \dots, x_l, \dots, x_n\}$ be the set of n objects, and $V = \{v_1, \dots, v_l, \dots, v_c\}$ be the set of c centroids in a p -dimensional feature space. The Fuzzy C-Means partitions X into c clusters by minimizing the following objective function [12]:

$$J = \sum_{j=1}^n \sum_{i=1}^c (\mathbf{u}_{ij})^m \|\mathbf{x}_j - \mathbf{v}_i\|^2 \quad (2)$$

where $1 \leq m \leq \infty$ is the *fuzzifier*; \mathbf{v}_j is the i^{th} centroid corresponding to cluster β_i ; $\mathbf{u}_{ij} \in [0, 1]$ is the fuzzy membership of the pattern \mathbf{x}_j to cluster β_i ; and $\|\cdot\|$ is the distance norm such that,

$$\mathbf{v}_i = \frac{1}{n_i} \sum_{j=1}^n (\mathbf{u}_{ij})^m \mathbf{x}_j \quad \text{where } n_i = \sum_{j=1}^n (\mathbf{u}_{ij})^m \quad (3)$$

and,

$$\mathbf{u}_{ij} = \frac{1}{\sum_{k=1}^c \left(\frac{d_{ij}}{d_{kj}}\right)^{\frac{2}{m-1}}} \quad \text{where } d_{ij}^2 = \|\mathbf{x}_j - \mathbf{v}_i\|^2 \quad (4)$$

FCM starts by randomly choosing c objects as centroids (means) of the c clusters. Memberships are calculated based on the relative distance (*i.e.* Euclidean distance) of the object \mathbf{x}_j to the centroids using (4). After the memberships of all objects have been found, the centroids of the clusters are calculated using (3). The process stops when the centroids

from the previous iteration are identical to those generated in the current iteration [12].

B. Type-II Fuzzy Sets

The main drawback with type-I fuzzy sets is that the assignment of a membership degree to an element (pixel) is not certain. Memberships are usually defined by the expert and are based on intuition and knowledge. The fact that different fuzzy techniques differ mainly in the way they define the membership function is for most of the part due to this dilemma [13]. Type-1 fuzzy sets are also not able to directly model uncertainties, since their membership functions are totally crisp. In order to find a more robust solution, type-II fuzzy sets should be introduced, as they are able to model uncertainties especially that their membership functions are themselves fuzzy [14]. Type-II fuzzy sets are fuzzy sets for which the membership function does not deliver a single value for every element, but an interval [13].

In order to define a type-II fuzzy set, one can define a type-I fuzzy set, and assign *upper* and *lower* membership degrees to each element in order to (re-)construct the footprint of uncertainty (FOU), which encapsulates the uncertainties associated with the membership functions, and is characterized by the upper and lower membership degrees μ_U and μ_L , respectively, of the initial (skeleton) membership function μ [13], [18].

Type-II fuzzy sets can be defined as [13]:

$$A^{\sim} = \{(x, \mu_U(x), \mu_L(x)) | \forall x \in X, \mu_L(x) \leq \mu(x) \leq \mu_U(x), \mu \in [0, 1]\} \quad (5)$$

The upper and lower membership values can be defined as [13]:

$$\mu_U(x) = [\mu(x)]^{\frac{1}{\alpha}} \quad (6)$$

$$\mu_L(x) = [\mu(x)]^{\alpha} \quad (7)$$

where $\alpha \in (1, \infty)$. For image data, $\alpha \in (1, 2]$ is recommended to be used, since $\alpha \gg 2$ is usually not meaningful for image data [13]. For our experimental results, $\alpha = 2$ was used.

C. Measure of Ultrafuzziness

The most common measure of fuzziness is the *linear index of fuzziness* [13]. We consider the CEUS image with type-II fuzzy sets, where the calculation of its degree of fuzziness is needed, provided that the higher the degree of fuzziness, the higher the image ambiguity, and thus, making the threshold definition difficult.

The measure of ultrafuzziness (*i.e.* linear index of fuzziness) γ^{\sim} for an $M \times N$ image subset $A^{\sim} \subseteq X$ with L gray levels $g \in [0, L-1]$, histogram $h(g)$, and the membership function $\mu_{A^{\sim}}(g)$, can be defined as [13]:

$$\gamma^-(A^-) = \frac{1}{MN} \sum_{g=0}^{L-1} h(g) \times [\mu_U(g) - \mu_L(g)] \quad (8)$$

where, $\mu_U(g)$ and $\mu_L(g)$ are defined in (6) and (7), respectively, and $\alpha \in (1, 2]$.

D. Calculating the Optimum Threshold Using Type-II Fuzzy Sets

The optimum threshold provides the global estimation of edge ambiguity. The general algorithm (Algorithm.1) for calculating the optimum threshold based on type-II fuzzy sets and measures of ultrafuzziness are as follows [13]:

Algorithm.1: Calculating the Optimum Threshold

- Select the shape of skeleton membership function $\mu(g)$ and initialize α ,
- Calculate the image histogram,
- Initialize the position of the membership function,
- Shift the membership function along the gray-level range,
- Calculate in each position the upper and lower membership values $\mu_U(g)$ and $\mu_L(g)$,
- Calculate in each position the amount of ultrafuzziness as in (8),
- Locate the position g_{opt} with maximum ultrafuzziness,
- Threshold the image with $T = g_{opt}$.

The membership function used in this paper is the *S-function* [15], which is defined as:

$$S(x; a, b, c) = \begin{cases} 0, & x \leq a; \\ \frac{1}{2} \left(\frac{x-a}{b-a} \right)^2, & a < x \leq b; \\ 1 - \frac{1}{2} \left(\frac{x-c}{c-b} \right)^2, & b < x \leq c; \\ 1, & x > c \end{cases} \quad (9)$$

where $a = 0, c = 1, b = \frac{a+c}{2} = 0.5$ (crossover point).

E. Defuzzification

In fuzzy clustering, the minimization of the functional J , given in (2), leads to partitions characterized by the membership degree matrix. A *defuzzification* is thus needed to obtain the final segmentation. Usually, the data is attributed to the class having the highest membership degree. In ultrasound imaging however, this method doesn't give appropriate results because lesion borders are often not clearly defined.

Boujemaa et al. [16] introduced the notion of local ambiguity for a given pixel by considering a spatial criterion, describing the neighborhood. The method is divided into two steps. Firstly, data are compared with the optimum threshold (calculated in the previous section) to reveal the most ambiguous pixels (*i.e.* weak membership degree) from the remaining strong ones (*i.e.* high membership degree) to

represent the coarse image information. In the second step, weak pixels are assigned with regards to their spatial context. As shown in Fig. 2, the weak pixel p_5 will be evaluated against its neighbors in the window (assuming the window is of size 3×3).

Each cluster (Fig. 3) could be represented by a crisp lower approximation, fuzzy boundary [12], core (*i.e.* $\mu_{ij} = 1$), and support (*i.e.* $\mu_{ij} > 0$).

p_1	p_2	p_3
p_4	p_5	p_6
p_7	p_8	p_9

Fig. 2 3×3 window

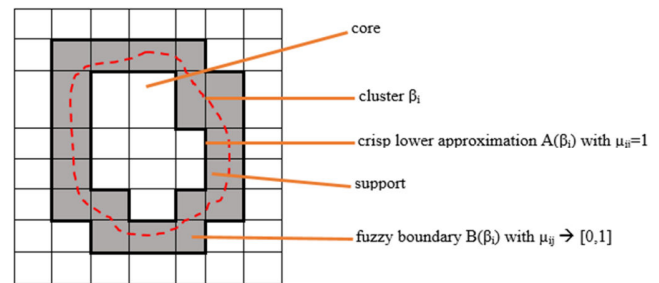


Fig. 3 Cluster β_i represented by a crisp lower approximation, fuzzy boundary, core, and support

To treat all ambiguous pixels, the whole image has to be explored. Different exploration methods are then possible. The first consists in making a *linear sweeping*, where the data is affected to the major cluster of its neighbors. Thus, in Fig. 4, the weak pixel will be assigned to cluster b .

a	c	b
b	p_5	b
c	b	a

Fig. 4 Weak pixel p_5 assigned to cluster b

Linear sweeping is a very fast method, but may affect ambiguous pixels to a class with several ambiguous neighbors. Obviously, it is frequent to deal with pixels which neighbors are also ambiguous. The second method is based on a double iterative sweeping in order to take a decision only with the less ambiguous pixels. This process is iterated until all pixels are treated. The first method was used in this paper.

The pseudocode for the proposed approach is demonstrated in Algorithm.2.

III. RESULTS AND DISCUSSION

The performance of the proposed approach was tested on six annotated liver contrast enhanced ultrasound (CEUS)

images, where the liver and the lesion areas were labeled by an expert. These images were obtained using a Siemens Acuson Sequoia 512 with a 4C1 probe, in CPS mode, after Sonovue injection. Fig. 5 shows a sample of such images, the ambiguous pixels that have been dealt with in the proposed approach (revealed and assigned to the appropriate clusters), the ground truth of the image sample, and the results obtained for three different methods.

Algorithm 2: Defuzzification by gradual focusing

Input /* image */
 $X = \{x_1, \dots, x_n\}$ /* set of n -objects (data points) */
 m /* number of classes */
Output
 $L = \{l_1, \dots, l_n\}$ /* l_i is a label for point x_i */
Implementation
 Matrix: μ /* membership matrix of size $n \times m$ */
Begin
Step 1 /* Initialization */
 Initialize the membership matrix μ with random values that satisfy the following constraints:
 $\mu_{ij} \in [0, 1], \forall_i = 1 \dots n, \forall_j = 1 \dots m$
 $\sum_{j=1}^m \mu_{ij} = 1, \forall_i = 1 \dots n$
Step 2
Repeat
 calculate the fuzzy centers $v_i, i=1..c$:

$$v_i = \frac{1}{n_i} \sum_{j=1}^n (\mu_{ij})^m x_j$$
 calculate the membership $\mu_{ij}, i=1..c, j=1..n$:

$$\mu_{ij} = \frac{1}{\sum_{k=1}^c \left(\frac{d_j}{d_{jk}}\right)^{\frac{2}{m-1}}}$$
 calculate the objective function J , until $J < \epsilon$:

$$J = \sum_{j=1}^n \sum_{i=1}^c (\mu_{ij})^m \|x_j - v_i\|^2$$
Step 3
 find ambiguous threshold β
Step 4 /* defuzzification */
for $i=1..n$
 $l_i = k$, where $\mu_{ik} = \max \mu_{ij}$
end
 /* reveal ambiguous pixels */
if $\mu_{ij} \geq \beta$
 assign pixel to its cluster
else if $\mu_{ij} < \beta$
 mark pixel as ambiguous
end
end
 /* check the neighborhood (i.e. 3×3) of the ambiguous pixels in order to assign them to the appropriate cluster */
if $\text{repeat}(c_m) > \text{repeat}(c_n)$
 assign pixel to c_m
else if $\text{repeat}(c_m) < \text{repeat}(c_n)$
 assign pixel to c_n
else if $\text{repeat}(c_m) == \text{repeat}(c_n)$
 assign pixel to cluster it would be appointed to in step 4
end
end
end
Return L

Step 5
 extract boundary of interest /* semi-automatic step for detecting the lesions */
End

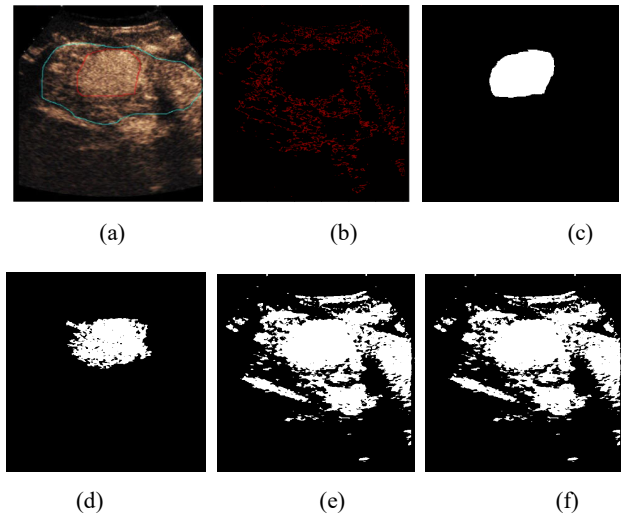


Fig. 5 (a) Annotated CEUS image (red region: lesion; green region: liver); (b) ambiguous pixels (in red); (c) ground truth of (a); (d) result of proposed approach; (e) Fuzzy C-Means clustering result; and (f) Otsu's method result

Table I shows the optimum threshold obtained for each CEUS image.

TABLE I
OPTIMUM THRESHOLD FOR EACH CEUS IMAGE

Image	Optimum threshold
1	0.0577
2	0.1164
3	0.0903
4	0.0638
5	0.1464
6	0.0604

We have studied six observation criteria [17], thereby highlighting the improvements in the segmentation, in terms of precision, shape and information extracted. We relied on precision, recall and the Dice index, all three defining statistically the quality of segmentation. We also analyzed the Hamming measure, which characterizes the number of disparities between two images. The shape analysis is based on the determination of the Mean Absolute Distance (denoted by MAD), and the SSIM (Structural SIMilarity) is used to estimate the amount of information extracted from the original image.

Precision and recall are defined as:

$$\text{Precision} = \frac{TP}{TP+FP} \tag{10}$$

$$\text{Recall} = \frac{TP}{TP+FN} \tag{11}$$

The Dice index is defined as:

$$\text{Dice index} = 2 \times \frac{\text{Precision} \times \text{Recall}}{\text{Precision} + \text{Recall}} \quad (12)$$

The *Manhattan distance* is defined as:

$$\text{Manhattan distance} = \frac{TP+TN}{TP+FP+TN+FN} \quad (13)$$

Hamming measure is defined as:

$$M_H(I_1 \Rightarrow I_2) = n - \sum_{R_2 \in I_2} \max_{R_1 \in I_1} |R_2 \cap R_1| \quad (14)$$

where R_1 and R_2 are segmentation areas in the images I_1 and I_2 , respectively. And, n is the number of pixels of one image.

The *mean absolute distance (MAD)*, which analyzes the contour points, and thus, the shape of the segmentation, is defined as:

$$\text{MAD}(R_1, R_2) = \frac{1}{M} \sum_{m=1}^M \|x_m - y_m\| \quad (15)$$

where x_m and y_m are contour points of R_1 and R_2 , respectively.

The *structural similarity (SSIM)* for the extracted structural information is defined as:

$$\text{SSIM}(R_1, R_2) = \frac{(2m_1m_2+k_1)(2cov_{1,2}+k_2)}{(m_1^2+m_2^2+k_1)(\sigma_1^2+\sigma_2^2+k_2)} \quad (16)$$

where m_1 and m_2 are the average values of R_1 and R_2 ; σ_1^2 and σ_2^2 are the *variance*; k_1 and k_2 are two coefficients proportional to the dynamic range of the pixel values.

Table II shows the results obtained for our approach, which uses the ambiguous pixels to delimitate its extraction, compared to Fuzzy C-Means clustering and Otsu's method [19].

From Table II, we can see that the proposed approach performs better compared to the two other methods. Indeed, the Dice index is increased by 10.57%, 10.81%, compared with Fuzzy C-Means clustering and Otsu's method, respectively. The number of disparities is divided by a factor of 10, and the criteria defining the shape and the information extracted is also improved. The shape of the segmentation is greatly enhanced and the quality of the information extracted increased by 42%. Figs. 5 (d)-(f) depict those results.

TABLE II
 SEGMENTATION PERFORMANCE OF THREE METHODS

	Proposed approach	FCM	Otsu
Precision	99.25%	99.91%	99.91%
Recall	98.65%	79.23%	78.85%
Dice index	98.95%	88.38%	88.14%
Hamming measure	5135	51157	52090
MAD	2.74	12.14	12.08
SSIM	0.88	0.61	0.62

IV. CONCLUSION

In obtaining the final segmentation from fuzzy clustering, a defuzzification (decision stage) is needed. Due to the complex nature of CEUS images, especially where lesion borders are often not clearly defined, the proposed approach used a two-

step decision stage: revealing ambiguous pixels, and assigning such ambiguous pixels to the appropriate clusters with regards to their spatial context. Dealing with and treating ambiguous pixels, through the proposed approach, provided significant improvements as compared to two classical segmentation algorithms, Fuzzy C-Means clustering, and Otsu's method. The proposed approach reduced the number of disparities, segmentation was enhanced, and the quality of the information extracted increased. As a future prospect to this work, we are aiming at expanding the proposed decision stage to be performed from a multi-scale decision perspective.

REFERENCES

- [1] H. Becher and P. Burns, "A Handbook of Contrast Echocardiography," Springer: Heidelberg, 2000.
- [2] E. Quiaia, A. Baert, and K. Sartot, "Contrast Media in Ultrasonography: Basic Principles and Clinical Applications," Springer, 2006.
- [3] A. Bouakaz, N. de Jong, and C. Cachard, "Standard Properties of Ultrasound Contrast Agents," *Ultrasound Med Biol* 24:469-472, 1998.
- [4] T. Albrecht, et al., "Guidelines for the Use of Contrast Agents in Ultrasound," *Ultraschall Med.* 25(4), pp.249-256, 2004.
- [5] J. Shan, "A Fully Automatic Segmentation Method for Breast Ultrasound Images," PhD thesis, Utah State University, 2011.
- [6] M.S. Yang, "A Survey of Fuzzy Clustering", *Math. Comput. Modelling* 18, 1-16, 1993. C. J. Kaufman, Rocky Mountain Research Lab., Boulder, CO, private communication, 1995.
- [7] Q. Williams and J. Noble, "A Spatio-temporal Analysis of Contrast Ultrasound Image Sequences for Assessment of Tissue Perfusion," *MICCAI 2004*:899-906, 2004.
- [8] R. Prevost, B. Mory, J.-M. Correias, L. D. Cohen, and R. Ardon, "Kidney Detection and Real-time Segmentation in 3D Contrast-enhanced Ultrasound Images," In *Proceedings of IEEE ISBI*, pages 1559-1562, 2012.
- [9] A. Albouy-Kissi, S. Cormier, and F. Tranquart, "Perfusion Quantification of Contrast-enhanced Ultrasound Images Based on Coherence Enhancing Diffusion and Competitive Clustering," *ICIP 2012*: 2321-2324. 2012.
- [10] A. Hassanieni, G. Schaefer, and H. Al-Qahri, "Prostate Boundary Detection in Ultrasounds Images based on Type-II Fuzzy Sets and Modified Fuzzy C-Means," *Soft Computing in Industrial Applications, Advances in Soft Computing*, 2010, Volume 75/2010, pp. 187-195, 2010.
- [11] H. Li, and M. Gupta, "Fuzzy logic and Intelligent systems." Kluwer Academic Publishers, 1995.
- [12] P. Maji and S. Pal. "Maximum Class Separability for Rough-Fuzzy C-Means Based Brain MR Image Segmentation," *T. Rough Sets*, Vol.9, pp.114-134, 2008.
- [13] H. Tizhoosh, "Image Thresholding Using Type II Fuzzy Sets," *Pattern Recognition*. 38(12), 2363-2372, 2005.
- [14] J. Mendel, R. John, "Type-2 Fuzzy Sets Made Simple," *IEEE Trans. Fuzzy Syst.* 10 (2), 117-127, 2002.
- [15] N. Sladoje, J. Lindbald, and I. Nyström, "Defuzzification of Discrete Objects by Optimizing Area and Perimeter Similarity," In: Kittler, J., Petrou, M., Nixon, M. (eds.) *Proc. of 17th International Conference on Pattern Recognition (ICPR 2004)*, Cambridge, UK, vol. 3, pp. 526-529. IEEE Comp. Society, Los Alamitos, 2004.
- [16] N. Boujemaa, G. Stamon, J. Lemoine, and E. Petit. "Fuzzy Ventricular Endocardium Detection with Gradual Focusing Decision," *14th Annual International Conference of the IEEE Engineering in Medicine and Biology Society*, Vol. 14, 1992.
- [17] M. Grand-Brochier, A. Vacavant, G. Cerutti, K. Bianchi, and L. Tougne, "Comparative Study of Segmentation Methods for Tree Leaves Extraction," In *ACM ICVS 2013, Workshop: VIGTA*, Saint Petersburg, Russia, 2013.
- [18] T. Chua and W. Tan, "Interval Type-2 Fuzzy System for ECG Arrhythmic Classification," *Fuzzy Systems in Bioinformatics and Computational Biology, Studies in Fuzziness and Soft Computing*. Volume 242, pp 297-314, 2009.
- [19] N. Otsu, "A Threshold Selection Method from Gray-level Histograms," *IEEE Trans. Sys., Man., Cyber.* 9(1): 62-66. doi:10.1109/TSMC.1979.4310076, 1979.